EXPERIMENTAL AND NUMERICAL STUDY OF A CONDENSING FLOW IN A DEVELOPING WALL JET

Paul B. Hoke, Wang Qingtian, John J. McGrath
Department of Mechanical Engineering
Michigan State University
East Lansing, MI 48824, USA

Bashar S. AbdulNour
Visteon Automotive Systems
Ford Motor Company
Plymouth, MI 48170, USA

ABSTRACT

An experimental and computational investigation of a developing ($0< x/w <10.8$), two-dimensional wall jet is presented for the following three steady-state situations: isothermal flow, flow past a cold wall in the absence of condensation and flow past a cold wall with condensation. Detailed velocity and temperature measurements are made using hot-wire as well as dual probe hot-wire/cold-wire anemometry. Local temperature compensation of hot-wire velocity measurements using a dual hot-wire/cold-wire probe was successfully implemented. The experimental results are compared with computational results for the first two cases using the computational fluid dynamics program FLUENT© 5.

For isothermal flow, the measured time-averaged stream-wise velocity distributions match previously reported data well. Neither the presence of a thermal gradient nor condensation significantly changed the measured time-averaged stream-wise velocity or the stream-wise normal stress distributions. In contrast, the non-dimensional, time-averaged temperature distribution across the jet was altered by the presence of condensation for the conditions studied.

The computational results reveal that both a realizable k-ε model and a Reynolds Stress Model (RSM) are able to predict the measured time-averaged, stream-wise velocity distributions well. The RSM reproduces the measured stream-wise normal stress more accurately than the k-ε model. Both CFD models are capable of predicting the measured time-averaged temperature distribution across the jet to within 6% of the temperature difference between the wall and the surroundings.

Future work will focus on the development of CFD models to predict condensation phenomena in developing jet flows for comparison with more detailed experimental data.

NOMENCLATURE

Re_w	Reynolds number based on jet slot width (U_{jet} w/ν)
SNS	Streamwise normal stress ($100\ (u'/U_{max})^2$)
T	Temperature (°C)
T_o	Wall temperature (°C)
T_{amb}	Ambient Temperature
U	Velocity (m/s)
U_{max}	Velocity maximum of jet (m/s)
U_{jet}	Velocity of inviscid core at jet exit
U^+	Velocity in wall coordinates (U/U_τ)
U_τ	Shear velocity at wall ($\sqrt{\nu\ dU(0)/dy}$)
u'	Root mean square (rms) of velocity time series (m/s)
u'^+	Velocity rms in wall coordinates (u'/U_τ)
w	Slot width
y^+	$y\ U_\tau/\nu$
θ	Non-dimensional temperature $(T-T_o)/(T_{amb}-T_o)$
δ_2	y location where $U = ½\ U_{max}$

EXPERIMENTAL FACILITY

An experimental facility (Figure 1) has been constructed to provide a two-dimensional wall jet flow field with controlled velocity, wall surface temperature and inlet humidity.

The facility is an open system that operates in suction mode to prevent disturbances created by the prime mover from entering the test chamber. Flow rate is adjusted with a throttle valve on the system exhaust and monitored by measuring the pressure drop across the upstream contraction.

The air flow is conditioned prior to entering the two dimensional contraction. The free stream turbulence intensity measured at the contraction inlet is approximately 2%. This conditioning provides a 2-D flow at the contraction exit with an inviscid core velocity that varies

spanwise by less than 2% and a turbulence intensity of 1.5% in the inviscid core of the flow.

The flow is humidified by injecting low pressure, low temperature steam into the inlet region of the duct. The duct is sufficiently long to homogenize the flow; temperature and humidity at the contraction exit are temporally stable within ±1.5 °C and ±4 %Rh after a start up transient period (approximately 5 minutes). The wall jet is spatially uniform to within 1 °C and 2 %Rh at any instant.

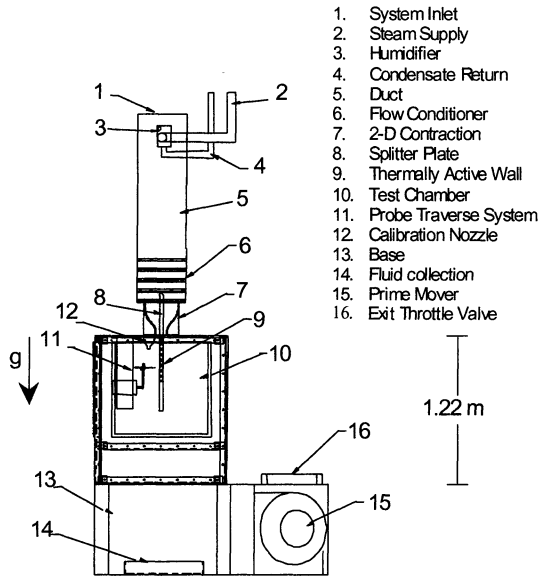

Figure 1. Experimental facility.

The thermally active wall surface is an aluminum heat exchanger with a baffled interior. A water-glycol mixture is pumped (0.25 l/s) through the heat exchanger by a constant temperature circulator bath. AbdulNour, et al. (1997) measured the surface temperature of this plate in a similar wall jet flow field and found that it varied by less than 0.4 °C over 80% of the surface (edge effects outside the utilized experimental area caused variations > 1 °C).

EXPERIMENTAL METHODS

Hot-wire anemometry and cold-wire resistance thermometry are utilized to measure the velocity and temperature profiles. The cold-wire measurement is utilized to temperature compensate the hot-wire in the thermally active experiments. The sensors are aligned parallel to the wall along the same spanwise axis. The active sections separated by 2mm. Both sensors are constructed on site from 5 μm diameter tungsten wire. A model 1050 TSI anemometer utilized to control the sensors and a 12 bit Keithley Metrabyte A/D card records their output at 1200 Hz. Experimental uncertainty is calculated as ± 0.25 m/s in the isothermal experiments and ± 0.35 m/s and ± 1 °C in the non-isothermal experiments. The sensor positions are controlled in 6 μm steps and are accurate within 25 μm.

Humidity is monitored with an Omega HX-11V humidity transducer in the duct upstream of the two dimensional contraction. The humidity transducer is accurate to ± 2% Rh.

Experimental uncertainty exceeds sensor resolution in each case.

WALL JET PARAMETERS

The study focuses on the developing region of a wall jet issuing from a rectangular slot (w = 2 cm) into a stagnant environment (Figure 2). Measurements of the velocity and temperature at non-dimensional streamwise locations from x/w = 0 to x/w = 10.8 are taken at Re_w = 13,000. This measurement regime encompasses the developing region of the momentum and thermal boundary layers from the slot exit to the onset of the fully-developed, self-preserving velocity profile.

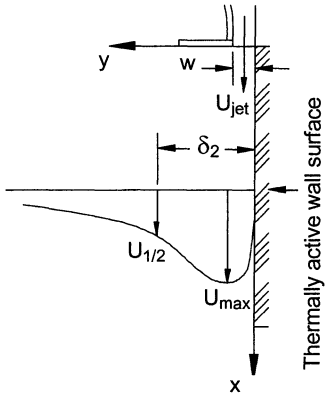

Figure 2. Wall jet definitions.

COMPUTATIONAL FLUID DYNAMICS SIMULATION

Model Geometry and Boundary Conditions

The experimental facility is modeled as a 2-D geometry and the boundary conditions are shown in Figure 3

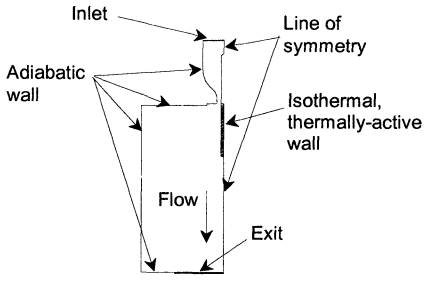

Figure 3. Boundary conditions for the numerical model.

The inlet and exit boundary conditions are specified as constant pressure with prescribed turbulence intensity. The isothermal wall is specified as either the ambient temperature (24 °C) for the isothermal tests or as the measured plate temperature (4 °C) for the non-isothermal tests. The other walls in the flow are modeled as adiabatic and impermeable. The centerline of the model above and below the splitter plate and isothermal plate utilizes symmetry boundary conditions.

The gauge pressure values at the inlet/outlet and the inlet turbulence intensity come directly from experimental measurements. The turbulence intensity at the exit is estimated.

CFD Simulation Methodology

A 2-dimensional, structured, quadrilateral mesh is generated from the geometry of the flow facility. The mesh contains 188,353 cells and is heavily clustered near the isothermal plate surface to improve resolution and accuracy in this region. The general-purpose CFD package FLUENT© 5 is used for the numerical simulation. The grid was adapted per the solution results in terms of y^+ and the velocity gradient. The y^+ dimension of the first computational node along the surface ranges from 0.975 to 1.23.

Turbulence Models and Near Wall Treatment

Both realizable k-ε and 5-equation Reynolds Stress Model (RSM) models are utilized in the simulation. The two models are chosen to compare a non-isotropic turbulence model (RSM) with an isotropic (k-ε) model in this flow field. FLUENT© applies explicit wall boundary conditions for the Reynolds stresses by using the log-law and the assumption of equilibrium, disregarding convection and diffusion in the transport equations for the stresses.

In favor of resolving the viscosity-affected near-wall region in the viscous sublayer, the two-layer zonal model is used for both realizable k-ε and RSM models. In this model, the wall functions are completely abandoned. The whole domain is subdivided into a viscosity-affected region and a fully-turbulent region in accordance with Re_y, defined based on wall-distance (y) and the turbulence kinetic energy (k).

$$Re_y = \frac{\sqrt{k}\, y}{\upsilon}$$

In the fully turbulent region ($Re_y > 200$), the k-ε model or the RSM are employed. In the viscosity-affected, near-wall region ($Re_y < 200$), a one-equation model is employed. The pressure-strain model is modified according to the two-layer zonal model for the RSM model in the near-wall region (Fluent, 1998).

RESULTS

Isothermal Flow Results

Comprehensive measurements of the isothermal flow are taken to provide baseline data for the wall jet development region and are compared to the CFD simulations. All figures in this paper contain all of the data for at least 4 time-averaged velocity measurements and the average result of 4 SNS measurements. The average of the SNS data is utilized to reduce clutter in the figures (each profile had a standard deviation of approximately ± 0.5). Figures 4 and 5 show the time-averaged velocity and the SNS profiles in the developing wall jet. Figure 4 shows the reduction of the inviscid core due to growth of the inner boundary layer and outer shear layer. Figure 5 shows increasing fluctuations near the wall and the inward propagation of the shear layer turbulence as the flow advances in the streamwise direction.

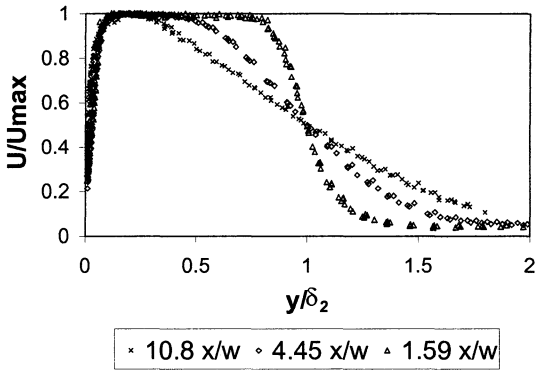

Figure 4. Velocity profiles in the wall jet development region (isothermal flow measurements).

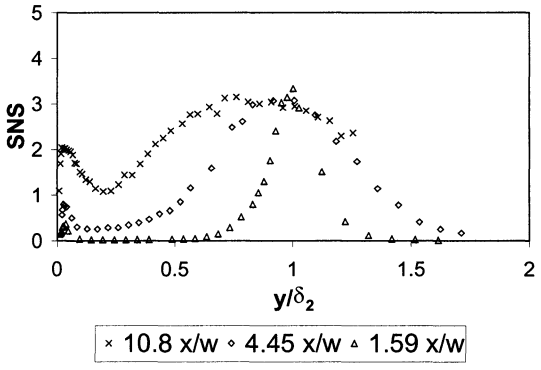

Figure 5. Streamwise normal stress profiles in the wall jet development region (isothermal flow measurements).

The data at the x/w = 10.8 position are compared to the results from other researchers to determine if a self-

preserving form is established. Figure 6 shows excellent agreement of the non-dimensional time-averaged velocity profile at x/w = 10.8 with the measurements of Tailland (1967) and Eriksson et al. (1997) at x/w = 600 and x/w = 20 respectively. It is concluded that the self-preserving velocity profile develops between the measurement locations of x/w = 7.62 and x/w = 10.8 in the current experiment.

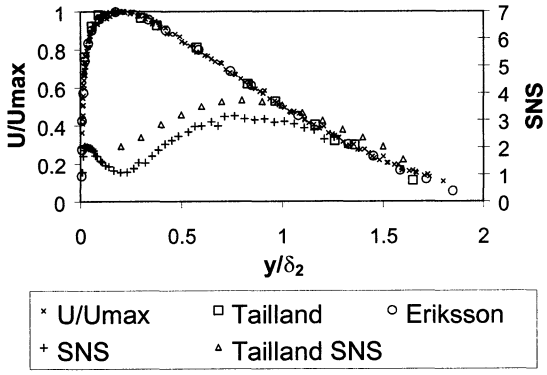

Figure 6. Comparison of x/w = 10.8 measurements with self preserving profiles.

The SNS profile measured at x/w = 10.8 is 20% to 30% lower than Tailland's data across the jet. Higher moments of the flow require longer to develop (Tennekes and Lumley, 1994). Therefore, it is not unexpected for the SNS profile to differ from measurements farther downstream. Tailland's SNS data are representative of the results compiled by Launder and Rodi (1981) which reveal 20% variation in magnitudes.

Figure 7 presents a wall coordinate comparison at x/w = 10.8 to data from Wygnanski et al. (1992) and to their Reynolds number (Re_w) dependent fit.

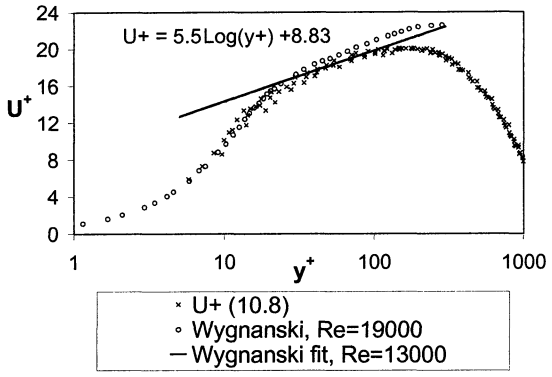

Figure 7. Velocity comparison in wall coordinates at x/w = 10.8 to data from Wygnanski et al.

The measured linear velocity gradient within 400 μm (y^+ < 12.5) of the surface is utilized to calculate the shear velocity. This includes 10 data points from 3 of the experiments. This is a second confirmation that the self-similar time-averaged velocity profile is developed and that the shear velocity measurement is consistent with other experiments.

Comparison to CFD simulation results. The isothermal measurements of the time-averaged velocity and the SNS are compared to the k-ε and RSM simulation results at x/w = 1.59 and 10.8 in Figures 8 and 9. The k-ε and the RSM models match almost identically in the time-averaged velocity plots in outer coordinates and are shown in the figures as a single line. The total velocity magnitude and the total velocity fluctuation are utilized for this comparison since the x and y velocity components are not distinguished by the experimental methodology (i.e. a single hot-wire is utilized). The k-ε and RSM models tend to over predict the thickness of the inner boundary layer.

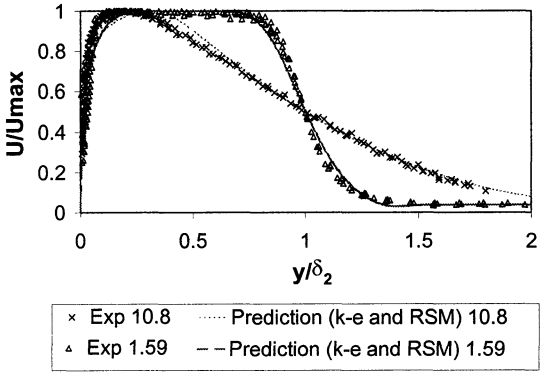

Figure 8. Time-averaged velocity comparison of experimental data and CFD predictions.

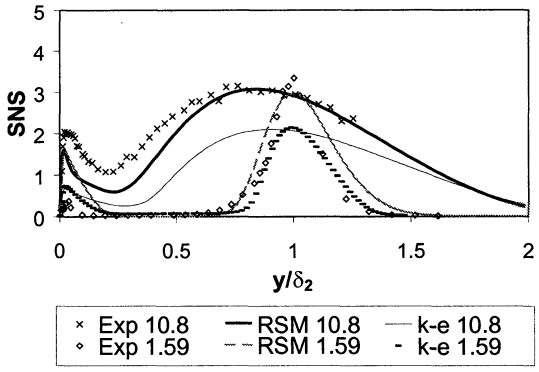

Figure 9. Steamwise normal stress comparison of experimental data and CFD predictions.

The k-ε and the RSM predictions of the time-averaged velocity agree closely with the experimental data (< 7.5%). The RSM model produces more accurate predictions of the SNS than the k-ε model (Figure 9). The RSM model predictions of the inner and outer peak SNS values are within 20% and 3% respectively of the measured data. Therefore the RSM results will be utilized for the remainder of the paper. The RSM model is decidedly superior in predicting turbulent quantities in the wall jet because there is no isotropy assumption built into the model.

Non-Isothermal Results

The non-isothermal tests and simulations are conducted with the isothermal plate temperature approximately 15 - 20 °C below ambient. This places the plate at or slightly below the saturation temperature. However, no condensation is observed during experiments.

The isothermal and non-isothermal velocity data are compared in Figure 10 and the non-isothermal temperature profiles are presented in Figure 11.

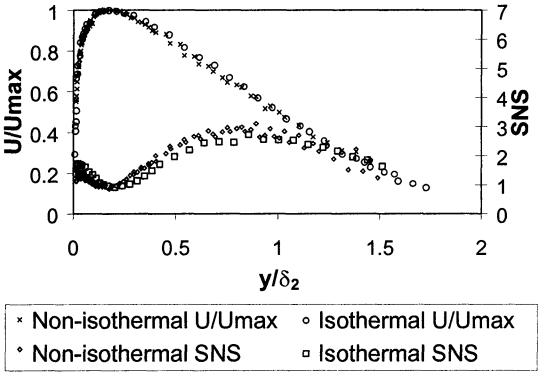

Figure 10. Comparison of isothermal and non-isothermal velocity measurements (x/w=10.8).

The velocity profiles are indistinguishable within the standard deviation of the measurements. This is expected due to the small changes in the physical properties over the temperature range utilized and a Grashoff–Reynolds number comparison which indicates that the inertial forces are several orders of magnitude greater than the buoyancy forces. SNS measurements agree very well with, and generally show less scatter than, the isothermal results. These results indicate that the temperature compensation of the hot-wire velocity measurements with the cold-wire measurement in the boundary layer is working properly.

The CFD simulations use a decoupled solution scheme to predict the velocity and temperature profiles. This is less computationally expensive and assumed to be acceptable since the experimentally measured velocity profile is unchanged by the presence of the temperature gradient.

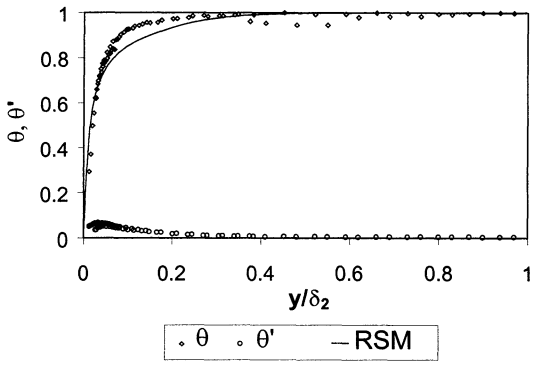

Figure 11. Comparison of experimentally measured and predicted (RSM model) temperature profiles (x/w = 10.8).

The match between the predicted and the measured temperature values is within 0.06 θ_{max}. The agreement between the predicted and measured profiles near the wall appears to be very good. Heat flux comparisons are not practical at this point due to the uncertainty in the measured temperature gradient.

Non-Isothermal, Condensing Results

The non-isothermal, condensing experiments are conducted with the isothermal wall temperature set at 4 °C and the relative humidity set at approximately 50% at the inlet. The ambient temperature is approximately 23 °C for all experiments. The time-averaged velocity profile is again expected to be unchanged due to the small changes in the fluid properties and the low rate of mass transfer associated with condensation. The experimental velocity measurements shown in Figure 12 bear out these expectations.

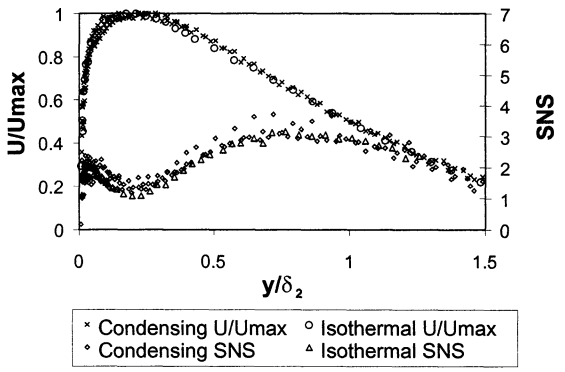

Figure 12. Comparison of velocity profiles in isothermal and non-isothermal, condensing experiments.

The data in Figure 13 reveal a difference in the temperature fields between the condensing and non-condensing experiments as large as 10% of the total temperature difference ($T_{max} - T_o$). These data are statistically different below $y/\delta_2 = 0.1$ at a 95% confidence level assuming that all the errors present are purely random. The cause and significance of this difference is currently unclear.

The current data are taken with a hot-wire and a cold-wire. The experiment ended when the hot-wire signal indicated failure. The reason for the hot wire failure is presently unknown, but this causes the current temperature measurement nearest to the wall to be at a y^+ location of approximately 10 (using the isothermal shear velocity).

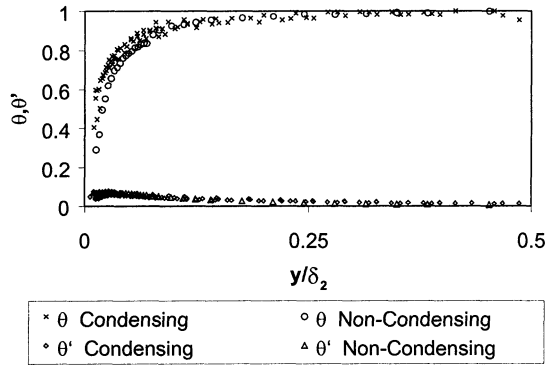

Figure 13. Comparison of temperature profiles in non-isothermal, non-condensing and non-isothermal, condensing experiments.

CONCLUSIONS

The following conclusions are supported by this research:

For the isothermal flow, the time-averaged stream-wise velocity distribution appears to reach the self-preserving form between $x/w = 7.62$ and 10.8, where the distribution matches previously reported data well.

Neither the presence of a thermal gradient nor condensation significantly changed the measured time-averaged stream-wise velocity or the SNS distributions

K-ε and RSM models predict virtually identical time-averaged, stream-wise velocity and temperature profiles in the developing region of a wall jet flow. The time-averaged velocity predictions differ from the experimental measurements by less than 8%. The time-averaged temperature predictions differ from the experimental measurements by less than 6%. The RSM model is clearly superior to the k-ε model in predicting the SNS. The RSM model predicts the SNS to within 20% throughout the jet and matches the peak value within 3%.

The cold-wire temperature measurement is utilized successfully to compensate the local hot-wire measurement within the boundary layer. This is demonstrated by the agreement of the measured mean velocity and SNS profiles in each thermally active experimental regime.

The differences between the temperature profiles in the condensing and non-condensing experiments are statistically difference in the near wall ($y/\delta_2 < 0.1$). The reason and significance of this difference are unclear at this time.

FUTURE WORK

Experiments to resolve the heat flux and velocity gradient at the wall are ongoing. This information will allow heat transfer comparisons to be made between the simulations and experiments in the non-isothermal cases.

Extension of the present steady-state situations to transient cases is of interest. Further detailed comparisons of numerical predictions and experimental data are planned. The long-term goal of this coordinated experimental and numerical effort is to develop and evaluate computational models that form the basis of design software for automotive fogging/defogging processes and devices.

REFERENCES

AbdulNour, R. S., Willenborg, K., McGrath, J. J., Foss, J. F., and AbdulNour, B.S., 1997, "Measurements of the Convective Heat Transfer Coefficient for a Two-Dimensional Wall Jet: Uniform Temperature and Uniform Heat Flux Boundary Conditions," HTD-Vol. 353, Proceedings of the ASME Heat Transfer Division, Volume 3, pp. 109-116.

Launder, B. E. and Rodi, W., 1981, "The Turbulent Wall Jet", Progress in Aerospace Science, Vol. 19, Pergamon Press, pp. 81-128.

Eriksson, J. G., Karlsson, R. I., and Persson, J., 1998, "An Experimental Study of a Two-Dimensional Plane Turbulent Wall Jet," Experiments in Fluids, Vol. 25, pp. 50-60.

Tennekes, H., and Lumley, J. L., 1994, A First Course In Turbulence, The MIT Press, Massachusetts, pp. 115.

Tailland, A., 1967, "Contribution à l'étude d'un jet plan dirigé tangentiellement à une paroi plane", Thése de Docteur es Sciences, Univ. Claude Bernard, Lyon.

Fluent Inc., 1998, FLUENT© 5 User's Guide; Volume 1-4, Lebanon, NH.

Wygnanski, I., Katz, Y., and Horev, E., 1992, "On the Applicability of Various Scaling Laws to the Turbulent Wall Jet," Journal of Fluid Mechanics, Vol. 234, pp. 669-690.

ACKNOWLEDGEMENTS

The authors wish to thank Dr. J.F. Foss and Dr. T. Shih at Michigan State University for their support. The authors also wish to acknowledge Dr. T. P. Gielda and Ford Motor Company for the financial support.